

On CRC-Aided, Dual-Trellis, List Decoding for High-Rate Convolutional Codes with Short Blocklengths

Wenhui Sui, *Student Member, IEEE*, Brendan Towell, *Student Member, IEEE*, Ava Asmani, *Student Member, IEEE*, Hengjie Yang, *Member, IEEE*, and Richard D. Wesel, *Fellow, IEEE*.

Abstract—Recently, rate- $1/n$ zero-terminated and tail-biting convolutional codes (ZTCCs and TBCCs) with cyclic-redundancy-check (CRC)-aided list decoding have been shown to closely approach the random-coding union (RCU) bound for short blocklengths. This paper designs CRCs for rate- $(n-1)/n$ CCs with short blocklengths, considering both the ZT and TB cases. The CRC design seeks to optimize the frame error rate (FER) performance of the code resulting from the concatenation of the CRC and the CC. Utilization of the dual trellis proposed by Yamada *et al.* lowers the complexity of CRC-aided serial list Viterbi decoding (SLVD) of ZTCCs and TBCCs. CRC-aided SLVD of the TBCCs closely approaches the RCU bound at a blocklength of 128. This paper also explores the complexity-performance trade-off for three decoders: a multi-trellis approach, a single-trellis approach, and a modified single trellis approach with pre-processing using the Wrap Around Viterbi Algorithm (WAVA).

I. INTRODUCTION

The structure of concatenating a convolutional code (CC) with a cyclic redundancy check (CRC) code has been a popular paradigm since 1994 when it was proposed in the context of hybrid automatic repeat request (ARQ) [2]. It was subsequently adopted in the cellular communication standards of both 3G [3] and 4G LTE [4]. In general, the CRC code serves as an outer error-detecting code that verifies if a codeword has been correctly received, whereas the CC serves as an inner error-correcting code to combat channel errors.

Recently, there has been a renewed interest in designing powerful short blocklength codes. This renewed interest is mainly driven by the development of finite blocklength information theory by Polyanskiy *et al.*, [5] and the stringent requirement of ultra-reliable low-latency communication (URLLC) for mission-critical IoT (Internet of Things) service [6]. In [5], Polyanskiy *et al.* developed a new achievability bound known as the random coding union (RCU) bound and a new converse bound, known as the meta-converse (MC) bound. Together, these two bounds characterize the error

probability range for the best short blocklength code of length N with M codewords. The URLLC for mission-critical IoT requires that the time-to-transmit latency is within $500 \mu s$ while maintaining a block error rate no greater than 10^{-5} .

Several short blocklength code designs have been proposed in the literature. Important examples include the tail-biting (TB) convolutional codes decoded using the wrap-around Viterbi algorithm (WAVA) [7], extended BCH codes under ordered statistics decoding [8], [9], non-binary low-density parity-check (LDPC) codes [10], non-binary turbo codes [11], and polar codes under CRC-aided successive-cancellation list decoding [12]. Recent advances also include the polarization adjusted convolutional codes by Arıkan [13]. As a comprehensive overview, Coşkun *et al.* [8] surveyed most of the contemporary short blocklength code designs in the recent decade. We refer the reader to [8] for additional information.

In [14], Yang *et al.* proposed the CRC-aided CCs as a powerful short blocklength code for binary-input (BI) additive white Gaussian noise (AWGN) channels. In [14], the convolutional encoder of interest has rate- $1/n$ and is either zero-terminated (ZT) or TB. In order to construct a good CRC-aided CC, Yang *et al.* selects a CC that maximizes its minimum distance and designs a *distance-spectrum optimal* (DSO) CRC generator polynomial for the given CC. The resulting concatenated code generated by the DSO CRC polynomial and the convolutional encoder is a good CRC-aided CC.

The nature of the concatenation naturally permits the use of the serial list Viterbi decoding (SLVD), an efficient algorithm originally proposed by Seshadri and Sundberg [15]. Yang *et al.* showed that the expected list rank of SLVD of the CRC-aided CC is small at high SNR where the target error probability is low, thus achieving a low average decoding complexity at the operating point of interest. Yang *et al.* demonstrated that several concatenated codes generated by the DSO CRC polynomial and the TBCC, or in short, CRC-TBCCs, approach the RCU bound. In [16], Schiavone extended this line of work by looking at the parallel list Viterbi decoding with a bounded list size. In our precursor conference paper [1], this framework is extended to rate- $(n-1)/n$ CCs and the resulting concatenated code is able to approach the RCU bound with a low decoding complexity as well.

In this paper, we present designs of good CRC-aided CCs for rate- $(n-1)/n$ CCs at short blocklengths for the BI-AWGN channel, where the CC is either ZT or TB. We consider systematic, rate- $(n-1)/n$ convolutional encoders. The resulting

This article was presented in part at the 2022 IEEE International Conference on Communications (ICC) [1].

This research is supported by National Science Foundation (NSF) under Grant CCF-2008918.

W. Sui, B. Towell, A. Asmani and R. D. Wesel are with the Department of Electrical and Computer Engineering, University of California, Los Angeles, Los Angeles, CA, 90095 USA (e-mail: wenhui.sui@ucla.edu; brendan.towell@ucla.edu; ava24@ucla.edu; wesel@ucla.edu).

Hengjie Yang is with Qualcomm Technologies, Inc., San Diego, CA 92121, USA (email: hengjie.yang@ucla.edu).

concatenated codes are respectively called a CRC-ZTCC and CRC-TBCC. We assume that SLVD has a sufficiently large list size such that no negative acknowledgement is produced. Thus, SLVD is an implementation of maximum-likelihood decoding. The frame error rate (FER) is in fact the undetected error probability. Simulations show that in the short-blocklength regime, our rate- $(n-1)/n$ CRC-TBCCs' performance is close to the RCU bound.

A work related to this line of research is that of Karimzadeh & Vu [17]. They considered designing the optimal CRC polynomial for multi-input CCs. In their framework, the information sequence is first divided into $(n-1)$ streams, one for each input rail, and they aim at designing optimal CRC polynomial for each rail. Unlike their architecture, in this paper, the information sequence is first encoded with a single CRC polynomial and is then divided into $(n-1)$ streams.

For rate- $(n-1)/n$ CCs, SLVD on the primal trellis requires high decoding complexity due to the 2^{n-1} outgoing branches at each node. SLVD implementation becomes exponentially more complicated when there are more than two outgoing branches per state. In order to simplify SLVD implementation and reduce complexity, we utilize the *dual trellis* pioneered by Yamada *et al.* [18]. The dual trellis expands the length of the primal trellis by a factor of n , while reducing the number of outgoing branches at each node from 2^{n-1} to at most two.

We consider two architectures to enforce the TB condition for CRC-TBCCs. One approach uses a single trellis with all initial states possible. At low SNR, SLVD on the single trellis requires a large list size to identify the ML TB codeword, with a majority of trellis paths not satisfying the TB condition. Since only one trellis is constructed in the forward pass and all tracebacks are conducted on this single trellis, it's impractical to enforce the TB condition when finding a new path. Therefore, we propose a new multi-trellis approach, where multiple copies of the dual trellis are initialized. Each trellis corresponds to a unique starting and ending state pair, therefore it is guaranteed that all paths found will be TB paths. This approach trades off the decoding time complexity of potentially exploring a large list size against the upfront overhead and space complexity for creating and storing multiple trellises. It can provide a benefit over the single-trellis approach when noise level is high.

Introduced in [19], WAVA is a near-maximum likelihood decoding algorithm for TBCCs. To achieve the balance of decoding time and space complexities, we propose an approach that combines the wrap-around behavior of WAVA with SLVD for TBCCs. The decoding process is completed in two steps: the WAVA step with at most 2 trellis iterations, and the list decoding step with a sufficiently large list size such that there is no negative acknowledgment signals. Simulation results demonstrate that this decoding method reduces the average list size as compared with the single-trellis decoder without WAVA, but this reduction comes at a cost of degraded FER performance.

A. Contributions

As a primary contribution, this work extends our previous work on high-rate CRC-CC list decoding with the dual trellis

[1] to further reduce the list size and decoding complexity. The original dual trellis approach, which uses the same tree-trellis algorithm to store the path metrics, suffers from a high average list rank at low SNRs. The novelty and contributions in this paper are summarized as follows:

- *Complexity comparison of three list decoders for TBCCs.*
 - An ML multi-trellis decoder that includes only TB codewords in the list of potential codewords by maintaining a distinct trellis for each starting state. We refer to this decoding scheme as the multi-trellis approach.
 - An ML decoder that avoids the complexity of having 2^v distinct trellises by using a single trellis but faces a potentially significant increase in list size by including both TB and non-TB paths in the list of potential transmitted codewords.
 - A sub-optimal (non-ML) decoder that lowers the list size of the single-trellis approach by using the wrap-around Viterbi algorithm (WAVA) to set the initial state metrics of the traceback trellis.
- *DSO CRC design for high-rate ZTCCs and TBCCs.*
 - This paper presents DSO CRC polynomial designs of various degrees for optimum rate-3/4 ZTCCs and TBCCs [20] in Table I and Table II. Formulated on the DSO CRC design algorithm for rate-1/n CCs [21], the design steps for high-rate include collecting the irreducible error events (IEEs), reconstructing all possible paths, and finally identifying the DSO CRC. These CRCs help reduce the gap between simulated SNR and the RCU bound.
 - This work compares the FER performance of a single DSO CRC and multiple shorter CRCs [22] for the same rate- $(n-1)/n$ ZTCCs, where the total CRC degrees of the two approaches are equal. The multi-CRC scheme assigns a different CRC for each of the $(n-1)$ input rails. Simulation results show that our framework can yield better FER performance than that of Karimzadeh & Vu.

B. Organization

The remainder of this paper is organized as follows. Sec. II reviews systematic encoding for $(n, n-1, v)$ convolutional codes, describes the dual trellis construction, and explains the tree-trellis algorithm for maintaining a list for trellis paths. Sec. III considers CRC-ZTCCs for rate- $(n-1)/n$ CCs. It addresses the zero-termination issue, presents DSO CRC design for high-rate ZTCCs, and shows CRC-ZTCC simulation results. Sec. IV considers CRC-TBCCs for rate- $(n-1)/n$ CCs. It addresses how to find the tail-biting initial state over the dual trellis and describes DSO CRC design for TBCCs. Additionally, Sec. IV introduces the multi-trellis decoder and WAVA decoder and analyzes the complexity and decoding performance of all three decoding schemes. Sec. V concludes the paper.

II. SYSTEMATIC ENCODING AND DUAL TRELLIS

This section describes systematic encoding for $(n, n-1, v)$ convolutional codes and introduces the dual trellis proposed

by Yamada *et al.* [18] for high-rate CCs generated with an $(n, n-1, v)$ convolutional encoder, where v represents the overall constraint length. This section also discusses the tree-trellis algorithm and its benefits.

A. Notation

Let K and N denote the information length and blocklength in bits. Let $R = K/N$ denote the rate of the CRC-aided CC. A degree- m CRC polynomial is of the form $p(x) = 1 + p_1x + \dots + p_{m-1}x^{m-1} + x^m$, where $p_i \in \{0, 1\}$, $i = 1, 2, \dots, m-1$. For brevity, a CRC polynomial is represented in hexadecimal when its binary coefficients are written from the highest to lowest order. For instance, 0xD represents $x^3 + x^2 + 1$. The codewords are BPSK modulated. The SNR is defined as $\gamma_s \triangleq 10 \log_{10}(A^2)$ (dB), where A represents the BPSK amplitude and the noise is distributed as a standard normal.

B. Systematic Encoding

We briefly follow [20, Chapter 11] in describing a systematic $(n, n-1, v)$ convolutional encoder. A systematic $(n, n-1, v)$ convolutional encoder can be represented by its parity check matrix

$$H(D) = [h^{(n-1)}(D), h^{(n-2)}(D), \dots, h^{(0)}(D)], \quad (1)$$

where each $h^{(i)}(D)$ is a polynomial of degree up to v in delay element D associated with the i -th code stream, i.e.,

$$h^{(i)}(D) = h_v^{(i)}D^v + h_{v-1}^{(i)}D^{v-1} + \dots + h_0^{(i)}, \quad (2)$$

where $h_j^{(i)} \in \{0, 1\}$. For convenience, we represent each $h^{(i)}(D)$ in octal form. For instance, $H(D) = [D^3 + D^2 + D + 1, D^3 + D^2 + 1, D^3 + D + 1]$ can be concisely written as $H = (17, 15, 13)$. Let $\mathbf{h}^{(i)} \triangleq [h_v^{(i)}, h_{v-1}^{(i)}, \dots, h_0^{(i)}]$, $i = 0, 1, \dots, n-1$. The systematic encoding matrix $G(D)$ associated with $H(D)$ is given by

$$G(D) = \begin{bmatrix} \frac{h^{(1)}(D)}{h^{(0)}(D)} & 1 & 0 & \dots & 0 \\ \frac{h^{(2)}(D)}{h^{(0)}(D)} & 0 & 1 & \dots & 0 \\ \vdots & \vdots & \vdots & \ddots & \vdots \\ \frac{h^{(n-1)}(D)}{h^{(0)}(D)} & 0 & 0 & \dots & 1 \end{bmatrix}. \quad (3)$$

The first output bit is a coded bit and the remaining output bits are a direct copy of the corresponding input bits.

C. Dual Trellis

The primal trellis associated with a rate- $(n-1)/n$ ZTCC has 2^{n-1} outgoing branches per state. Performing SLVD over the primal trellis when $n > 2$ is highly complex. In [21], the low decoding complexity of SLVD for rate- $1/n$ convolutional codes relies on the fact that only 2 outgoing branches are associated with each state. In order to efficiently perform SLVD, we consider the dual trellis proposed by Yamada *et al.* [18].

We briefly explain the dual trellis construction for parity check matrix $H(D) = [h^{(n-1)}(D), h^{(n-2)}(D), \dots, h^{(0)}(D)]$. First, we define the maximum instant response order λ as

$$\lambda \triangleq \max\{j \in \{0, 1, \dots, n-1\} : h_0^{(j)} = 1\}. \quad (4)$$

The state of the dual trellis is represented by the partial sums of $(v+1)$ adders in the observer canonical form of $H(D)$. At time index j , $j = 0, 1, \dots, n-1$, the state is given by

$$\mathbf{s}^{(j)} = [s_v^{(j)}, s_{v-1}^{(j)}, \dots, s_0^{(j)}]. \quad (5)$$

Next, we show how the state $\mathbf{s}^{(j)}$ evolves in terms of the output bits $\mathbf{y}_k = [y_k^{(0)}, y_k^{(1)}, \dots, y_k^{(n-1)}]$, $k = 1, 2, \dots, N/n$, so that a dual trellis can be established.

Dual trellis construction for $\mathbf{y}_k = [y_k^{(0)}, y_k^{(1)}, \dots, y_k^{(n-1)}]$:

- 1) At time $j = 0$, $\mathbf{s}^{(0)} = [0, s_{v-1}^{(j)}, s_{v-2}^{(j)}, \dots, s_0^{(j)}]$, where $s_i^{(0)} \in \{0, 1\}$. Namely, only 2^v states exist at $j = 0$.
- 2) At time j , $j < n-1$, draw branches from each state $\mathbf{s}^{(j)}$ to state $\mathbf{s}^{(j+1)}$ by

$$\mathbf{s}^{(j+1)} = \mathbf{s}^{(j)} + y_k^{(j)} \mathbf{h}^{(j)}, \quad y_k^{(j)} \in \{0, 1\}. \quad (6)$$

- 3) At time $j = n-1$, draw branches from each state $\mathbf{s}^{(n-1)}$ to state $\mathbf{s}^{(n)}$ by

$$\mathbf{s}^{(n)} = \left(\mathbf{s}^{(n-1)} + y_k^{(n-1)} \mathbf{h}^{(n-1)} \right)^r, \quad y_k^{(n-1)} \in \{0, 1\}, \quad (7)$$

where $(a_v, a_{v-1}, \dots, a_1, a_0)^r = (0, a_v, a_{v-1}, \dots, a_1)$.

- 4) For time $j = \lambda$, draw a branch from each state $\mathbf{s}^{(\lambda)}$ according to (6) only for $y_k^{(\lambda)} = s_0^{(\lambda)}$.

After repeating the above construction for each \mathbf{y}_k , $k = 1, 2, \dots, N/n$, we obtain the dual trellis associated with the $(n, n-1, v)$ convolutional code. Since the primal trellis is of length N/n , whereas the dual trellis is of length N , the dual trellis can be thought of as expanding the primal trellis length by a factor of n , while reducing the number of outgoing branches per state from 2^{n-1} to less than or equal to 2.

D. Tree-Trellis Algorithm

SLVD enumerates possible paths through the trellis, starting from the lowest weight path, stopping once the first path that satisfies both the CRC and the TB condition is reached. Thus recordings of previously investigated path metrics are required to find the next optimal path. Inserting or accessing an element in an unsorted list of path metrics can substantially increase the time complexity of an algorithm.

To efficiently perform SLVD on the dual trellis, we used the tree-trellis algorithm (TTA) proposed by Soong and Huang in [23]. The TTA maintains a sorted list of nodes which are indexed by path metric. These nodes either correspond to a previously unexplored ending state in the trellis, or to a previously explored path and a detour. This approach allows the efficient determination of the next path to be explored if the current one does not satisfy both the CRC and TB condition.

This algorithm maintains a sorted list, which can become expensive if not implemented with an efficient data structure. In [24], the authors used Red-Black tree [25] to maintain the sorted list of nodes. In this paper, we use a Min Heap [26],

TABLE I
DSO CRC POLYNOMIALS FOR RATE-3/4 ZTCC AT BLOCKLENGTH
 $N = 128$ GENERATED BY $H = (33, 25, 37, 31)$ WITH $v = 4$, BY
 $H = (47, 73, 57, 75)$ WITH $v = 5$, AND BY $H = (107, 135, 133, 141)$
WITH $v = 6$

K	m	R	$v = 4$ CRC	$v = 5$ CRC	$v = 6$ CRC
87	3	0.680	0x9	0x9	0xB
86	4	0.672	0x1B	0x15	0x1D
85	5	0.664	0x25	0x25	0x25
84	6	0.656	0x4D	0x7B	0x6F
83	7	0.648	0xF3	0xED	0x97
82	8	0.641	0x1E9	0x1B7	0x1B5
81	9	0.633	0x31B	0x3F1	0x2F1
80	10	0.625	0x5C9	0x66F	0x59F
79	11	0.617	0xC2B	0xE8D	0xD2D

which is easier to implement and has the same $\mathcal{O}(\log n)$ time complexity to maintain the properties of its structure. A Min Heap is a complete binary tree that often underpins practical priority queue implementations. It requires no space overhead over a standard array. It provides constant-time minimum element access and logarithmic-time deletion of the minimum element. Insertion of a new element is logarithmic-time in the worst case, but constant-time on average. Constant average insertion time helps control overall average time complexity because insertion is the dominant operation performed by the decoder. Every path searched requires only accessing and removing the minimum node, and all detours along that path are inserted into the heap as nodes.

III. ZTCC WITH DSO CRC VIA DUAL TRELLIS SLVD

This section considers CRC-ZTCCs for rate- $(n-1)/n$ CCs. Section III-A presents a zero termination method over the dual trellis. Section III-B describes our DSO CRC polynomial search procedure. Finally, Section III-C presents simulation results of the CRC-ZTCC compared with the RCU bound. As a case study, this paper mainly focuses on the rate-3/4 systematic feedback convolutional codes in [20, Table 12.1(e)].

A. Zero Termination of Dual Trellis

For an $(n, n-1, v)$ CC, zero termination over the dual trellis requires at most $n\lceil v/(n-1) \rceil$ steps. In our implementation, a breadth-first search identifies the zero-termination input and output bit patterns that provide a trajectory from each possible state s to the zero state. The input and output bit patterns have lengths $(n-1)\lceil v/(n-1) \rceil$ and $n\lceil v/(n-1) \rceil$ respectively.

B. Design of DSO CRCs for High-Rate ZTCCs

In general, a DSO CRC polynomial provides the optimal distance spectrum which minimizes the union bound on the FER at a specified SNR [21]. In this paper, we focus on the low FER regime. Thus, the DSO CRC polynomials identified in this paper simply maximize the minimum distance of the concatenated code. Examples in [21] indicate that DSO CRC polynomials designed in this way can provide optimal or near-optimal performance for a wide range of SNRs.

The design procedure of the DSO CRC polynomial for high-rate ZTCCs essentially follows from the DSO CRC design

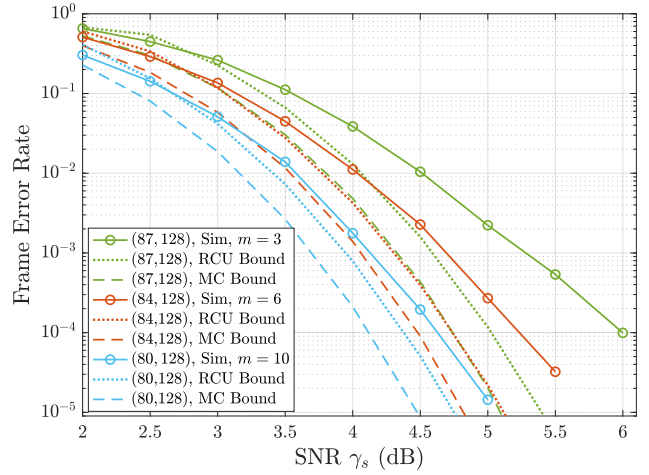


Fig. 1. FER vs. SNR for various CRC-ZTCCs. The ZTCC is generated with the $(4, 3, 6)$ encoder $H = (107, 135, 133, 141)$. The DSO CRC polynomials of degrees 3, 6, and 10 are 0xB, 0x6F, and 0x59F, respectively. Values in parenthesis denote information length K and blocklength N , respectively.

algorithm for low target error probability in [21]. The first step is to collect the IEEs, which are ZT paths on the trellis that deviate from the zero state once and rejoin it once. IEEs with a very large output Hamming weight do not affect the choice of optimal CRCs. In order to reduce the runtime of the CRC optimization algorithm, IEEs with output Hamming weight larger than a threshold $\tilde{d} - 1$ are not considered. Dynamic programming constructs all ZT paths of length equal to N/n and output weight less than \tilde{d} . Finally, we use the resulting set of ZT paths to identify the degree- m DSO CRC polynomial for the rate- $(n-1)/n$ CC.

Table I presents the DSO CRC polynomials for ZTCCs generated with $H = (33, 25, 37, 31)$, $H = (47, 73, 57, 75)$, and $H = (107, 135, 133, 141)$. The design assumes a fixed blocklength $N = 128$ bits. Due to the overhead caused by the CRC bits and by zero termination, the rates of CRC-ZTCCs are less than 3/4. Specifically, for a given information length K , CRC degree m and an $(n, n-1, v)$ encoder, the blocklength N for a CRC-ZTCC is given by

$$N = \left(K + m + (n-1) \left\lceil \frac{v}{n-1} \right\rceil \right) \frac{n}{n-1}, \quad (8)$$

giving

$$R = \frac{K}{N} = \frac{n-1}{n} \frac{K}{K + m + (n-1) \left\lceil \frac{v}{n-1} \right\rceil}. \quad (9)$$

We see from (8) that the $(n, n-1, v)$ convolutional encoder can accept any CRC degree m as long as $K + m$ is divisible by $(n-1)$.

C. Results and Comparison with RCU Bound

Fig. 1 shows the performance of CRC-ZTCCs with increasing CRC degrees 3, 6 and 10 and a fixed blocklength $N = 128$ bits. We see that at the target FER of 10^{-4} , increasing the CRC degree reduces the gap to the RCU bound. With $m = 10$ and $v = 6$, the CRC-ZTCC approaches the RCU bound within 0.25 dB.

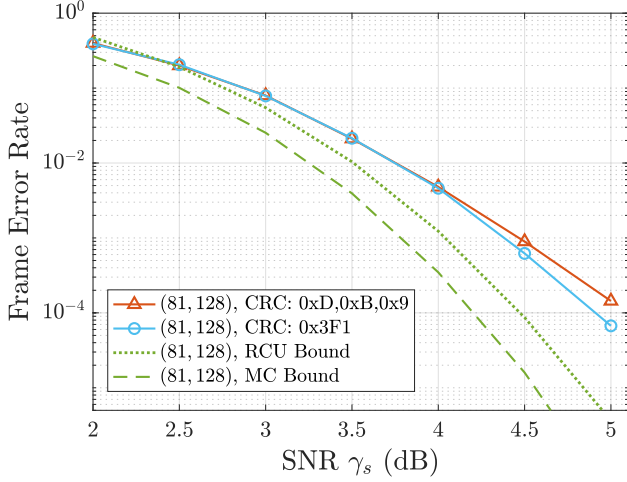


Fig. 2. FER vs. SNR for $v = 5$ CRC-ZTCCs designed under Karimzadeh *et al.*'s scheme [17] and our scheme. Both CRC-ZTCCs have information length $K = 81$ and blocklength $N = 128$.

In [17], Karimzadeh *et al.* considered designing optimal CRC polynomials for each input rail of a multi-input CC. In their setup, an information sequence for an $(n, n-1, v)$ encoder needs to be split into $(n-1)$ subsequences before CRC encoding. In contrast, the entire information sequence in our framework is encoded with a single CRC polynomial. Then the resulting sequence is evenly divided into $(n-1)$ subsequences, one for each rail. To compare the performance between these two schemes, we design three degree-3 optimal CRC polynomials, one for each rail, for ZTCC with $H = (47, 73, 57, 75)$. The three CRC polynomials jointly maximize the minimum distance of the CRC-ZTCC. For the single-CRC design, we use the single degree-9 DSO CRC polynomial for the same encoder from Table I. Both CRC-ZTCCs have an information length $K = 81$ and blocklength $N = 128$. Fig. 2 shows the performance comparison between these two codes, showing that a single degree-9 DSO CRC polynomial outperforms three degree-3 DSO CRC polynomials, one for each rail. This suggests that a single DSO CRC polynomial may suffice to provide superior protection for each input rail. The decoding complexity is similar regardless of the CRC scheme.

IV. TBCC WITH DSO CRC AND DUAL TRELLIS SLVD

The performance of CRC-aided list decoding of ZTCCs relative to the RCU bound is constrained by the termination bits appended to the end of the original message, which are required to bring the trellis back to the all-zero state. TBCCs avoid this overhead by replacing the zero termination condition with the TB condition, which states that the final state of the trellis is the same as the initial state of the trellis [27].

In this section, we apply SLVD to CRC-TBCCs over the dual trellis. Section IV-A demonstrates designs of DSO CRCs for rate $(n-1)/n$ TB codes. In section IV-B, we will discuss how to determine the initial state for the TBCC to ensure that the TB condition is met on a single dual trellis. Detailed discussion about the construction of the multi-trellis decoder and WAVA decoder and their benefits are presented in sections

TABLE II
DSO CRC POLYNOMIALS FOR RATE-3/4 TBCC AT BLOCKLENGTH $N = 128$ GENERATED BY $H = (33, 25, 37, 31)$ WITH $v = 4$, BY $H = (47, 73, 57, 75)$ WITH $v = 5$, AND BY $H = (107, 135, 133, 141)$ WITH $v = 6$

K	m	R	$v = 4$ CRC	$v = 5$ CRC	$v = 6$ CRC
93	3	0.727	0x9	0x9	0xB
92	4	0.719	0x1B	0x1D	0x17
91	5	0.711	0x25	0x3B	0x33
90	6	0.703	0x7D	0x4F	0x41
89	7	0.695	0xF9	0xD1	0xBD
88	8	0.688	0x1CF	0x173	0x111
87	9	0.680	0x38F	0x3BF	0x333
86	10	0.672	0x73F	0x697	0x723

IV-C and IV-D, respectively. Finally, the decoding complexity and performance are analyzed in sections IV-E and IV-F.

A. Design of DSO CRCs for High-Rate TBCCs

The design of DSO CRCs for high-rate TBCCs follows the two-phase design algorithm shown in [21]. This algorithm is briefly explained below.

Consider a TB trellis $T = (V, E, \mathcal{A})$ of length N , where \mathcal{A} denotes the set of output alphabet, V denotes the set of states, and E denotes the set of edges described in an ordered triple (s, a, s') with $s, s' \in V$ and $a \in \mathcal{A}$ [28]. Assume $|V| = 2^v$ and let $V_0 = \{0, 1, \dots, 2^v - 1\}$. Define the set of IEEs at state $\sigma \in V$ as

$$\text{IEE}(\sigma) \triangleq \bigcup_{l=1,2,\dots,N} \overline{\text{IEE}}(\sigma, l), \quad (10)$$

where

$$\begin{aligned} \overline{\text{IEE}}(\sigma, l) \triangleq \{(\mathbf{s}, \mathbf{a}) \in V_0^{l+1} \times \mathcal{A}^l : s_0 = s_l = \sigma; \\ \forall j, 0 < j < l, s_j \notin \{0, 1, \dots, \sigma\}\}. \end{aligned} \quad (11)$$

The IEEs at state σ can be thought of as “building blocks” for an arbitrarily long TB path that starts and ends at the same state σ .

The first phase is called the collection phase, during which the algorithm collects $\text{IEE}(\sigma)$ with output Hamming weight less than the threshold \tilde{d} over a sufficiently long TB trellis. The second phase is called the search phase, during which the algorithm first reconstructs all TB paths of length N/n and output weight less than \tilde{d} via concatenation of the IEEs and circular shifting of the resulting path. Then, using these TB paths, the algorithm searches for the degree- m DSO CRC polynomial by maximizing the minimum distance of the undetected TB path.

Table II presents the DSO CRC polynomials for TBCCs generated with $H = (33, 25, 37, 31)$, $H = (47, 73, 57, 75)$, and $H = (107, 135, 133, 141)$. The design assumes a fixed blocklength $N = 128$. TB encoding avoids the rate loss caused by the overhead of the zero termination. Specifically, for a given information length K , CRC degree m and an $(n, n-1, v)$ encoder, the blocklength N for a CRC-TBCC is given by

$$N = (K + m) \frac{n}{n-1}, \quad (12)$$

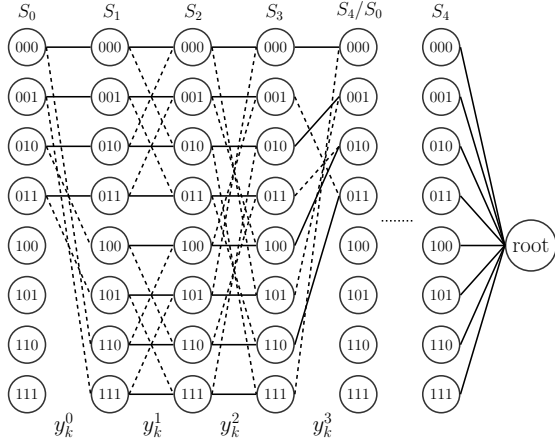


Fig. 3. Dual trellis diagram for rate-3/4 TBCC with a root node at the end for encoder $H = (2, 5, 7, 6)$ with $v = 2$. Solid lines represent 0 paths and dashed lines represent 1 paths.

giving

$$R = \frac{K}{N} = \frac{n-1}{n} \frac{K}{K+m}. \quad (13)$$

B. Single Trellis List Decoding for CRC-TBCC

There are two primary differences in the development and analysis of list decoding between ZTCCs, as described in Section III, and TBCCs. One difference is that since the ZT condition is replaced with the TB condition, the encoder must determine the initial trellis state so that the TB condition is satisfied. The other difference is that SLVD on the dual trellis must be adapted to handle the TB condition.

To satisfy the TB condition, encoding is attempted from every initial state to identify the initial state that satisfies the TB condition. This is required because our recursive encoder cannot simply achieve the TB condition by setting the initial encoder memory to be the final bits of the information sequence.

To adapt SLVD on the dual trellis to handle the TB condition, we propose an efficient way to keep track of the path metrics and find the next path with minimum metric through an additional root node as shown in Fig. 3. The root node connects to all terminating states after forward traversing the dual trellis. The Hamming distance of the branch metric for the branch connecting any state to this root node is zero. This additional root node allows the trellis to end in a single state, so that the basic SLVD approach for a ZTCC may be applied. During SLVD, if the current path does not pass either the CRC or TB check, the minimum value among all remaining path metrics will be selected as the next path to check.

C. Multi-Trellis List Decoding for CRC-TBCC

Decoding on a single dual trellis (single-trellis approach) leads to complexity issues, since a large sorted list is maintained to keep track of all possible traceback paths – but not all of them will satisfy the TB condition. Thus the decoder will go through a number of paths that pass neither the TB check or CRC, resulting high expected list ranks at low SNRs. To

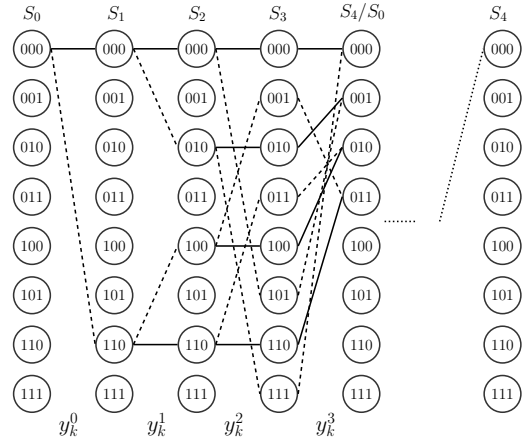


Fig. 4. Multi-trellis construction for rate-3/4 TBCC dual trellis with encoder $H = (2, 5, 7, 6)$ with $v = 2$. The pictured trellis has starting and ending state of 0. Three similar trellises are also constructed for this encoder with starting and ending states of 1-3.

decode more efficiently, we propose an multi-trellis approach in this section.

As its name indicated, the multi-trellis approach requires construction of 2^v dual trellises, since only half of the states in a dual trellis are valid starting and ending states. As shown in Fig. 4, each multi-trellis follows the same structure as a dual trellis, but with only one starting and ending state to enforce the TB condition. For example, for the encoder $H = (2, 5, 7, 6)$ with $v = 2$, there are $2^2 = 4$ multi-trellises for this encoder. The final root node is also removed.

An obvious advantage of using the multi-trellis approach is that all the paths found will be tail-biting. This greatly reduces the expected list size compared to the single-trellis approach at low SNRs. However, at high SNRs, the multi-trellis approach has a substantially higher decoding complexity due to the additional upfront cost of constructing the dual trellises. In this case, the extra resources taken to initialize the multi-trellis approach brings down the overall decoder efficiency.

D. List Decoding with WAVA

As the constraint length of a TBCC increases, the number of states grows exponentially. The multi-trellis approach becomes impractical due to both time and memory for constructing the trellises. Thus, we adopt a non-ML decoder with WAVA to improve the decoding efficiency while maintaining a reasonable decoding complexity. Proposed in [19], the WAVA decodes TB trellises iteratively and is able to effectively reduce the expected list rank. An initial examination of the list size distributions for the three decoding schemes at SNR = 2 dB is presented in Fig.5 on a $v = 4$ TBCC. While the multi-trellis approach outperforms the other approaches with an extremely small list size at all times, the WAVA approach still has a substantially larger probability of a small list size compared to the single-trellis. Different distributions lead to different $E[L]$ and $E[L]$ values when evaluating the decoding complexity.

The non-ML decoder with WAVA proceeds in two steps. In the first step, the algorithm initializes each state of a single dual trellis with all zero metrics. It then performs two iterations

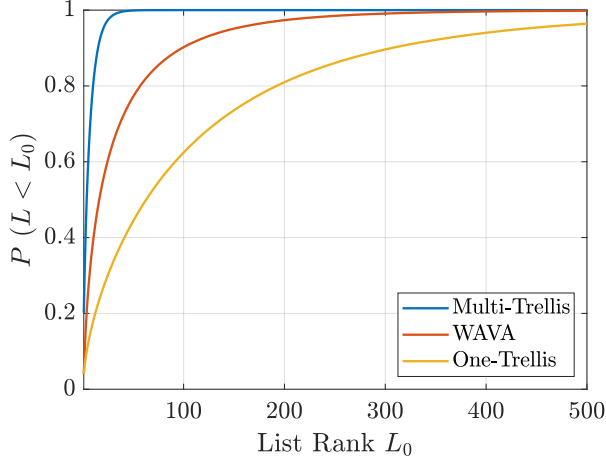


Fig. 5. Cumulative distribution function (CDF) of list ranks for the single-trellis, multi-trellis, and WAVA decoding approaches for the (33, 25, 37) TBCC with blocklength of 128 at SNR = 2 dB.

of add-compare-select (ACS) along the trellis; each time the end of the trellis is encountered, the initial states of the trellis are initialized to the cumulative metrics in the final states. At the end of the first iteration, if the optimal path satisfies TB and CRC conditions, the algorithm outputs this path and stops decoding. In the second step, SLVD runs on the ending metrics of the second trellis iteration. This decoding algorithm improves the reliability of the final decision for the optimal traceback path and decreases the expected list rank while keeping the complexity low. However, this algorithm is non-optimal, thus it has a slightly worse decoding performance than the other two ML approaches.

E. Complexity Analysis

In [21], the authors provided the complexity expression for SLVD of CRC-ZTCCs and CRC-TBCCs, where the convolutional encoder is of rate $1/n$. Observe that the dual trellis has no more than 2 outgoing branches per state, similar to the trellis of a rate- $1/n$ CC. Thus, we directly apply their complexity expression to SLVD over the dual trellis.

As noted in [21], the overall average complexity of SLVD can be decomposed into three components:

$$C_{\text{SLVD}} = C_{\text{SSV}} + C_{\text{trace}} + C_{\text{list}}, \quad (14)$$

where C_{SSV} denotes the complexity of a standard soft Viterbi (SSV), C_{trace} denotes the complexity of the *additional* traceback operations required by SLVD, and C_{list} denotes the average complexity of inserting new elements to maintain an ordered list of path metric differences.

C_{SSV} is the complexity of ACS operations and the initial traceback operation. For CRC-ZTCCs,

$$C_{\text{SSV}} = (2^{v+1} - 2) + 1.5(2^{v+1} - 2) + 1.5(K + m - v)2^{v+1} + c_1[2(K + m + v) + 1.5(K + m)]. \quad (15)$$

For CRC-TBCCs decoded using the single-trellis, this quantity is given by

$$C_{\text{SSV}} = 1.5(K + m)2^{v+1} + 2^v + 3.5c_1(K + m). \quad (16)$$

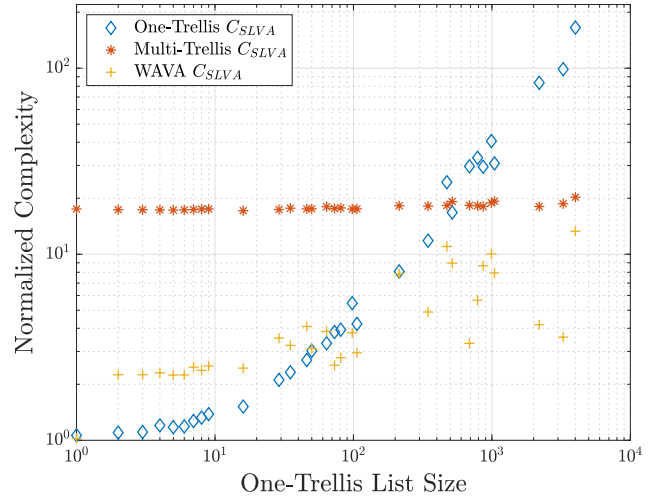


Fig. 6. The overall complexity comparison of the single-trellis, multi-trellis, and WAVA decoders for the TBCC generated with the (4, 3, 4) encoder $H = (33, 25, 37)$, with blocklength of 128. The CRC polynomial of degree 3 is 0x9. All complexity values are normalized with respect to the single-trellis C_{SSV} at different list sizes.

For CRC-TBCCs with the multi-trellis approach,

$$C_{\text{SSV}} = 2^v[1.5(K + m)2^{v+1}] + 3.5c_1(K + m). \quad (17)$$

The second component C_{trace} for CRC-ZTCC is given by

$$C_{\text{trace}} = c_1(E[L] - 1)[2(K + m + v) + 1.5(K + m)]. \quad (18)$$

For CRC-TBCCs, C_{trace} is given by

$$C_{\text{trace}} = 3.5c_1(E[L] - 1)(K + m), \quad (19)$$

for both single-trellis and multi-trellis approaches.

The third component, which is identical for ZT and TB, is

$$C_{\text{list}} = c_2 E[I] \log(E[I]), \quad (20)$$

where $E[I]$ is the expected number of insertions to maintain the sorted list of path metric differences. For CRC-ZTCCs,

$$E[I] \leq (K + m)E[L], \quad (21)$$

and for CRC-TBCCs with either single-trellis or multi-trellis approach,

$$E[I] \leq (K + m)E[L] + 2^v - 1. \quad (22)$$

In the above expressions, c_1 and c_2 are two computer-specific constants that characterize implementation-specific differences in the implemented complexity of traceback and list insertion (respectively) as compared to the ACS operations of Viterbi decoding. In this paper, we assume that $c_1 = c_2 = 1$ and use (21) and (22) to estimate $E[I]$ for CRC-ZTCCs and CRC-TBCCs, respectively.

Note that $E[I]$ and $E[L]$ values vary depending on whether the single-trellis or multi-trellis approach is used. Using the multi-trellis approach significantly reduces C_{trace} and C_{list} because only TB paths are included. On the other hand, as seen from (16) and (17), the multi-trellis approach amplifies the first component C_{SSV} by nearly 2^v . The overall tradeoff is depicted in Fig. 6, which shows the complexity comparison

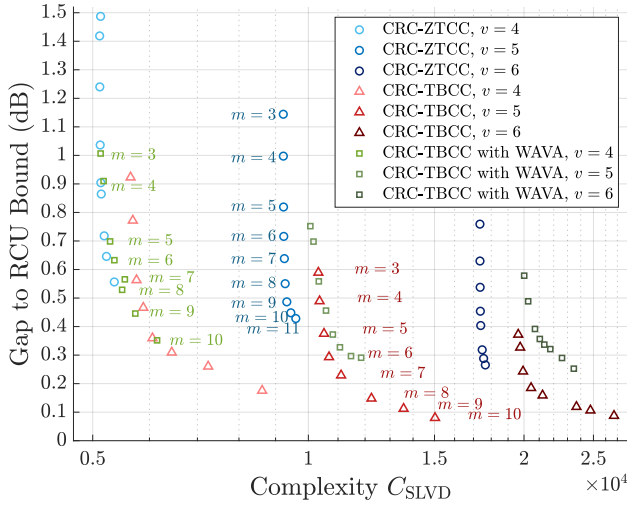


Fig. 7. The SNR gap to the RCU bound vs. the average complexity of SLVD of CRC-ZTCC codes in Table I and CRC-TBCC codes in Table II for target FER of 10^{-4} . For CRC-TBCCs, results for both single-trellis decoding and WAVA decoding are demonstrated. Each color represents a specific CRC-aided CC shown in the tables. Markers from top to bottom with the same color correspond to DSO CRC polynomials with $m = 3, \dots, 10$ for TBCCs, and $m = 3, \dots, 11$ for ZTCCs.

of the single-trellis and multi-trellis approach on a $v = 4$ TBCC with a $m = 3$ CRC. Various random codewords with blocklength $N = 128$ are generated and their single-trellis list sizes are measured by passing through a single-trellis SLVD with TB checks and CRCs. The runtime of each complexity component is normalized with respect to the value of single-trellis C_{SSV} . When the single-trellis list size is 1, the overall runtime of the multi-trellis approach is over 10 times of that of the single-trellis approach, due to the overhead complexity of constructing multiple trellises. At low noise level, the list size of a single trellis is 1 for the most time, resulting in a substantially lower runtime compared to that of a multi-trellis. As SNR decreases, the list size of the single-trellis decoder grows larger, leading to an exponential growth in the complexity terms C_{trace} and C_{list} . Although the multi-trellis C_{list} term also has an increasing trend, that value is small compared to the term C_{trace} . Because the construction of the trellis structure mainly contributes to the complexity of multi-trellis, at different SNR levels the complexity maintains the same magnitude. At a list size of around 5×10^2 , the overall runtime C_{SLVD} of both approaches become the same. This indicates that at high SNR level, single-trellis is the optimal approach as the list size is low. But in cases where the noise level is high, the multi-trellis approach is guaranteed to satisfy the TB condition, thus it provides a reduced runtime regardless of its complex construction.

Upon applying WAVA, the overall average complexity for CRC-TBCC is incremented by ACS operations during the additional forward pass, if needed. Let the probability that the optimal path of the initial traceback does not satisfy either TB or CRC condition be P_{WAVA} . The list rank of the decoder is 1 with a probability of $1 - P_{WAVA}$. Thus we have the updated

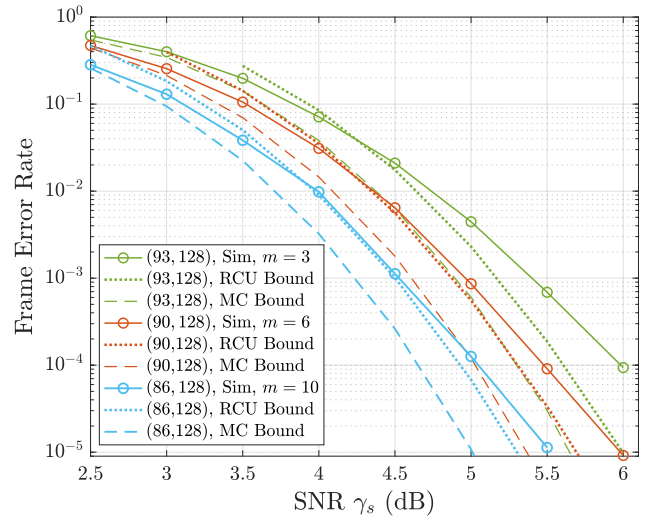


Fig. 8. FER vs. SNR for various CRC-TBCCs. The TBCC is generated with the $(4, 3, 6)$ encoder $H = (107, 135, 133, 141)$. The DSO CRC polynomials of degrees 3, 6, and 10 are 0xB, 0x41, and 0x723, respectively. Values in parenthesis denote information length K and blocklength N , respectively.

complexity:

$$C_{SLVD} = C_{SSV} + P_{WAVA} \times (C_{WAVA} + C_{trace} + C_{list}), \quad (23)$$

where

$$C_{WAVA} = 1.5(K + m)2^{v+1} + 2^v. \quad (24)$$

The yellow data points in Fig.6 represent the overall complexity of the WAVA decoder normalized with respect to the single-trellis C_{SSV} at various list sizes. The complexity for initializing the WAVA decoder is about 2 times of that for the single-trellis, giving it an disadvantage at low noise levels. However, at a list size of exactly 1, due to the traceback after the first iteration, the WAVA decoder matches the complexity of the single-trellis decoder. At a list size of around 5×10^1 , the overall complexity of the WAVA decoder reaches the same level as the single-trellis decoder. In addition, the WAVA decoder operates at a complexity lower than the multi-trellis decoder.

F. Results, Analysis, and Expected List Rank of SLVD

Fig. 7 shows the trade-off between the SNR gap to the RCU bound and the average decoding complexity at the target FER 10^{-4} for CRC-ZTCCs designed in Table I and CRC-TBCCs designed in Table II. The average decoding complexity of SLVD is evaluated according to the expressions in Sec. IV-E. We see that for a fixed v (ZT or TB), increasing the CRC degree m significantly reduces the gap to the RCU bound, at the cost of a small increase in complexity. The minimum gap of 0.08 dB is achieved by the CRC-TBCC with $v = 5$ and $m = 10$. However, for the same CRC degree m , increasing the overall constraint length v dramatically increases the complexity, while achieving a minimal reduction in the SNR gap to the RCU bound. For CRC-TBCCs, the WAVA decoder has a slightly larger gap to RCU bound than the single-trellis decoder due to the extra ACS operations during the first traceback. However, the complexity of the WAVA

decoder is smaller than that of the single-trellis decoder, and the difference increases as the CRC degree increases. For all constrain lengths v , the WAVA decoder at $m = 10$ has a similar complexity as the single-trellis decoder at $m = 7$.

Additionally, the performance of CRC-ZTCC can be improved drastically by applying CRCs of higher degrees. Fig. 7 demonstrates that for all three cases of constraint lengths v , one additional bit in the CRC benefits the decoding performance by moving closer to the RCU gap with a minimal cost in complexity. Thus at a gap to RCU bound for around 0.4 dB, CRC-ZTCC outperforms CRC-TBCC by a substantially reduced decoding complexity.

Fig. 8 shows the FER vs. SNR for three CRC-TBCCs at blocklength $N = 128$. At the target FER of 10^{-4} , the SNR gap to the RCU bound is reduced to 0.1 dB for the CRC-TBCC with $m = 10$ and $v = 6$.

V. CONCLUSION

This paper shows that high-rate CRC-aided CCs are able to approach the RCU bound for the BI-AWGN channel. The best CRC-TBCCs with the single-trellis ML decoder approach the RCU bound within 0.1 dB for a target FER of 10^{-4} at a blocklength of $N = 128$ bits.

This paper considers three decoding algorithms for rate- $(n-1)/n$ CCs concatenated with DSO CRC polynomials: a multi-trellis approach, a single-trellis approach, and a modified single trellis approach with pre-processing using the Wrap Around Viterbi Algorithm (WAVA). All three algorithms use the dual trellis to reduce complexity. The multi-trellis approach achieves the smallest expected list rank, but it suffers from a significantly larger overall complexity than the single-trellis approach. For the single trellis approach, we considered both an ML decoder and a non-ML decoder that uses WAVA pre-processing. WAVA pre-processing achieves a significantly smaller expected list size than the ML single-trellis decoder, but the non-ML decoder achieves a slightly worse FER performance. In addition, adding one bit to the CRC can improve the FER far more than adding an additional memory element to the CC does for all three approaches. In the future, it will be interesting to investigate and compare the performance and complexity of a parallel list Viterbi decoder (PLVD) on high-rate CC-CRC codes.

REFERENCES

- [1] W. Sui, H. Yang, B. Towell, A. Asmani, and R. D. Wesel, "High-rate convolutional codes with crc-aided list decoding for short blocklengths," in *ICC 2022 - IEEE International Conference on Communications*, 2022, pp. 98–103.
- [2] M. Rice, "Comparative analysis of two realizations for hybrid-ARQ error control," in *1994 IEEE Global Commun. Conf.*, 1994, pp. 115–119.
- [3] "Universal mobile telecommunications system (UMTS); multiplexing and channel coding (FDD); 3GPP TS 25.212 version 7.0.0 release 7," European Telecommunications Standards Institute, Tech. Rep., 2006.
- [4] "LTE; evolved universal terrestrial radio access (E-UTRA); multiplexing and channel coding; 3GPP TS 36.212 version 15.2.1 release 15," European Telecommunications Standards Institute, Tech. Rep., 2018.
- [5] Y. Polyanskiy, H. V. Poor, and S. Verdú, "Channel coding rate in the finite blocklength regime," *IEEE Trans. Inform. Theory*, vol. 56, no. 5, pp. 2307–2359, May 2010.
- [6] H. Ji, S. Park, J. Yeo, Y. Kim, J. Lee, and B. Shim, "Ultra-reliable and low-latency communications in 5G downlink: Physical layer aspects," *IEEE Wireless Commun. Mag.*, vol. 25, no. 3, pp. 124–130, 2018.

- [7] L. Gaudio, T. Ninacs, T. Jerkovits, and G. Liva, "On the performance of short tail-biting convolutional codes for ultra-reliable communications," in *SCC 2017; 11th Int. ITG Conf. Syst., Commun., and Coding*, Feb. 2017, pp. 1–6.
- [8] M. C. Coşkun, G. Durisi, T. Jerkovits, G. Liva, W. Ryan, B. Stein, and F. Steiner, "Efficient error-correcting codes in the short blocklength regime," *Physical Commun.*, vol. 34, pp. 66 – 79, 2019.
- [9] C. Yue, M. Shirvanimoghaddam, B. Vucetic, and Y. Li, "A revisit to ordered statistics decoding: Distance distribution and decoding rules," *IEEE Trans. Inform. Theory*, vol. 67, no. 7, pp. 4288–4337, 2021.
- [10] L. Dolecek, D. Divsalar, Y. Sun, and B. Amiri, "Non-binary protograph-based LDPC codes: Enumerators, analysis, and designs," *IEEE Trans. Inform. Theory*, vol. 60, no. 7, pp. 3913–3941, 2014.
- [11] G. Liva, E. Paolini, B. Matuz, S. Scalise, and M. Chiani, "Short turbo codes over high order fields," *IEEE Trans. Commun.*, vol. 61, no. 6, pp. 2201–2211, 2013.
- [12] I. Tal and A. Vardy, "List decoding of polar codes," *IEEE Trans. Inform. Theory*, vol. 61, no. 5, pp. 2213–2226, 2015.
- [13] E. Arkan, "From sequential decoding to channel polarization and back again." [Online]. Available: <http://arxiv.org/abs/1908.09594>
- [14] H. Yang, E. Liang, M. Pan, and R. D. Wesel, "CRC-aided list decoding of convolutional codes in the short blocklength regime," *ArXiv*, vol. abs/2104.13905, 2021.
- [15] N. Seshadri and C. E. W. Sundberg, "List Viterbi decoding algorithms with applications," *IEEE Trans. Commun.*, vol. 42, no. 234, pp. 313–323, Feb. 1994.
- [16] R. Schiavone, "Channel coding for massive IoT satellite systems," Master's thesis, Politecnico University of Turin (Polito), 2021.
- [17] M. Karimzadeh and M. Vu, "Optimal CRC design and serial list Viterbi decoding for multi-input convolutional codes," in *2020 IEEE Global Commun. Conf.*, 2020, pp. 1–6.
- [18] T. Yamada, H. Harashima, and H. Miyakawa, "A new maximum likelihood decoding of high rate convolutional codes using a trellis," *Elec. and Commun. in Japan Part I-commun.*, vol. 66, pp. 11–16, 1983.
- [19] R. Shao, S. Lin, and M. Fossorier, "Two decoding algorithms for tailbiting codes," *IEEE Transactions on Communications*, vol. 51, no. 10, pp. 1658–1665, 2003.
- [20] S. Lin and D. J. Costello, *Error Control Coding: fundamentals and applications*. New Jersey, USA: Pearson Prentice Hall, 2004.
- [21] H. Yang, E. Liang, M. Pan, and R. D. Wesel, "Crc-aided list decoding of convolutional codes in the short blocklength regime," *IEEE Transactions on Information Theory*, vol. 68, no. 6, pp. 3744–3766, 2022.
- [22] M. Karimzadeh and M. Vu, "Optimal crc design and serial list Viterbi decoding for multi-input convolutional codes," in *GLOBECOM 2020 - 2020 IEEE Global Communications Conference*, 2020, pp. 1–6.
- [23] F. Soong and E.-F. Huang, "A tree-trellis based fast search for finding the n-best sentence hypotheses in continuous speech recognition," in *ICASSP 91: 1991 International Conference on Acoustics, Speech, and Signal Processing*, 1991, pp. 705–708 vol.1.
- [24] M. Roder and R. Hamzaoui, "Fast tree-trellis list Viterbi decoding," *IEEE Trans. Commun.*, vol. 54, no. 3, pp. 453–461, Mar. 2006.
- [25] R. Hinze, "Constructing red-black trees," 10 1999.
- [26] A. Hasham, "A new class of priority queue organizations," Master's thesis, 1986, aAI0662089.
- [27] H. Ma and J. Wolf, "On tail biting convolutional codes," *IEEE Trans. Commun.*, vol. 34, no. 2, pp. 104–111, Feb. 1986.
- [28] R. Koetter and A. Vardy, "The structure of tail-biting trellises: minimality and basic principles," *IEEE Trans. Inform. Theory*, vol. 49, no. 9, pp. 2081–2105, Sep. 2003.